Assessing structural bonding aspects of multiband superconductors through impurity-induced local lattice distortions: a case study on MgB_2

Aleksandr Pishtshev[1] **and Mihhail Klopov**[2]

[1] Institute of Physics, University of Tartu, Riia 142, 51014 Tartu, Estonia

E-mail: aleksandr.pishtshev@ut.ee

[2] Department of Physics, Faculty of Science, Tallinn University of Technology, Ehitajate 5, 19086 Tallinn, Estonia

E-mail: mihhail.klopov@ttu.ee

Abstract. We report the results of an ab initio modeling of substitutional impurities such as zinc, copper and zirconium ions incorporated into the magnesium sublattice of MgB_2. These species are of particular interest because they demonstrate the lowest-observed-droop of the superconducting temperature among most of the impurities of the same formal valences. The goal of computational studies was to gain an atomistic understanding of how the structural and bonding properties of the local ionic environment are affected by a change in the host cation. The simulations performed for the given set of substituents indicate that at a low doping level, the induced lattice distortions and additional forces are noticeable small. At the same time, the electron redistributions around the impurities have been found to differ drastically both from that around the host cation and from each other. Results of the first-principles calculations were used to compare and discuss, in the context of the cation properties, specific changes in local charge structures and in chemical bonding caused by the presence of the impurity. Certain trends in substituent effects were found. It was determined how the substitutional ion modifies the initial charge distribution around the host cation position and therefore, affects both the overall picture of the electronic states involved in the chemical bonding and the intrinsic charge-transfer channels. Our studies demonstrate that the robust structural stability of the boron sublattice of MgB_2, which preserves the nearest-neighbor environment around the B atoms practically unchanged from an impurity incorporation into the magnesium site, has important functional significance – it supports a much weaker dependence of the superconducting temperature on impurity content. The present work gives insight into structural and electronic features of the impurity caused-processes which contribute to unique material properties of various MgB_2-solid solutions.

PACS numbers: 71.15.Mb, 74.62.Dh, 74.70.Ad

1. Introduction

In a theoretical analysis of impurity signatures, principally important is the fact that the equilibrium between the (nearest neighbors) lattice atoms, and the implanted impurity atom represents the structural balance between local geometry and chemical bonding, which depends strongly on the interatomic distances. In order to explore the dynamical nature of substituent effects on small length scales one can employ an approach based on a detailed atomistic view: it can be straightforwardly implemented within ab-initio numerical simulations, which are able to calculate the relative ionic displacements and the charge density redistribution accompanying the effect of the substitution. The results of calculations will then allow us both to capture the final binding geometry around the impurity site and to answer the fundamental question as to what extent the impurity atom is capable of adapting itself to the local environment and the existing chemical bonds.

In this paper, we apply such integrative approach to investigate the effects of substitutions for several 3d transition-metal impurities such as divalent Cu(II), Zn(II) and tetravalent Zr(IV) in magnesium diboride MgB_2. We consider MgB_2 containing substitutions of Mg as a doped model system for which we perform a series of the relevant numerical simulations. There are two reasons that make this system attractive for detailed study. First, while different properties of magnesium diboride doped by a variety of impurity atoms have been extensively studied in the past decade, the investigation of impurities in this material is still a topical subject, raising a number of actual issues that are worthy of special attention (for details see [1, 2, 3, 4, 5, 6, 7, 8, 9, 10, 11, 12], and the references cited therein). The other reason is that knowledge on how the arrangement of a single impurity ion influences on a local structural order may have useful predictive value in the rational design of magnesium diboride solid solutions. One of those issues, which is especially important to all aspects of local geometry and stability, is the influence of substitutions on a principal atomic configuration and the bonding properties of the cation environment. However, in many cases, information on the bonding situation around a substitutional impurity turns out to be limited, and there remain several questions about binding of metal elements incorporated into the place of the host Mg(II) cation. Understanding the latter is very essential because the response of the system on doping is not clear *a priori*. For example, it was experimentally established that the suppression of the superconducting properties proceeds much slower in the Zn-, Cu- and Zr-doped systems, as compared to compounds that contain other dopant ions of the same formal valences (details can be found in [1, 4, 6, 9, 11, 13]). In table 1, using the data available from the literature, we have summarized some examples related to this observation.

From the rate of decrease of the superconducting temperature T_c with chemical substitution of the original Mg with metal elements in MgB_2 one can expect that not all the impurity properties are matched well with those of Mg. Thus, the given example of table 1 shows that conceptually Zn-, Cu- and Zr-containing solutions stand among

Table 1. Experimental lowering of the T_c value (ΔT_c) in the $M_xMg_{1-x}B_2$ compositions at substitution levels (x) in the range $0.03 < x < 0.10$.

M	Zn	Cu	Zr	Ca	Co	Fe	Ni	Pb
$x : \Delta T_c$	$0.03 : -0.2$[a]	$0.03 : 0.5$[c]	$0.05 : 0.5$[e]	$0.03 : 0.5$[g]	$0.03 : 2.8$[h]	$0.03 : 5.1$[i]	$0.03 : 2.9$[i]	$0.03 : 1.5$[j]
	$0.05 : 0.5$[b]	$0.05 : 0.2$[d]	$0.05 : 0.7$[f]	$0.05 : 1.2$[g]	$0.03 : 2.0$[i]	$0.05 : 8.5$[i]	$0.05 : 4.8$[i]	$0.05 : 1.8$[j]
	$0.10 : 0.2$[b]		$0.10 : 1.1$[f]	$0.07 : 1.8$[g]	$0.05 : 3.3$[i]			$0.07 : 2.2$[j]

[a][14]; [b][15]; [c][16]; [d][17]; [e][18]; [f][19]; [g][20]; [h][21]; [i][11]; [j][22]

other doped systems as a particular example. This feature prompted us to examine in more detail the role of these substitutional ions and ion-specific effects in the context of impurity-induced changes in local structure, dynamics and chemical bonding. Therefore, the aim of the present paper is by employing ab initio calculations to study variations of certain lattice and charge characteristics, such as lattice distortions, interatomic forces, charge densities and bonding features, caused by compositional variations in MgB_2. By comparative analysis of features of the impurity atom with those related to the host one we pay attention in our work to what is happening within an ionic environment in the elementary cell when an intensity of interionic and electronic correlations is affected by the replacements of a magnesium cation.

2. Computational details and impurity simulation

According to the literature data (e.g., [1, 4, 23]), a crystalline structure of the bulk MgB_2 consists of alternating honeycomb layers of B interleaved with closed packed layers of Mg. Each Mg atom is located at the center of a hexagon formed by boron; by donating two valence electrons it becomes a strongly charged ion with a charge very close to +2. Consensus on the nature of the superconductivity in MgB_2 is based on a generic multiband model which employs the intra- and interband pair-scattering mechanisms. The presence of the interband channel connecting the σ and the π electronic bands [24, 25, 26] gives rise to a unique property of MgB_2 - two-gap superconductivity, which is characterized by two gaps of different sizes that are simultaneously closed at the same temperature T_c of the superconducting transition.

The first-principles modeling of the effects of Mg(II) ion substitutions in the $M_xMg_{1-x}B_2$ compositions, where M stands for a transition metal cation such as Zn, Cu or Zr, was performed using the Vienna Ab-initio Simulation Package (VASP) [27, 28, 29, 30] in conjunction with a plane-wave-basis code and the projector-augmented wave (PAW) method [31, 32]. Exchange-correlation effects were described through the Perdew-Burke-Ernzerhof (PBE) framework [33]. For geometry optimization, one of the host atoms was replaced by one M element in a 81-atoms supercell ($3 \times 3 \times 3$). Such arrangement shown in figure 1 corresponds to $x = 0.037$ in terms of the formal stoichiometry of the doped system. The lattice distortion caused by the substitution

has the following features: (1) it is totally symmetric on the cation site, and (2) it involves displacements of 12 nearest-neighbor boron atoms from regular positions. For a central boron atom, these displacements lead in turn to local symmetry breaking. Full relaxation of atomic positions was made with periodic boundary conditions and theoretical (structurally relaxed) bulk lattice parameters. The convergence criteria for total energy and residual forces calculations were set to be within 1×10^{-3} eV/atom and 1×10^{-3} eV/Å, respectively. A cut-off energy of 700 eV and a Monkhorst-Pack k-point grid [34] of $5 \times 5 \times 5$ has been employed. This computational scheme was successfully tested by a comparison of the calculated values of the lattice constants, $a_{calc} = 3.069$ Å; $c_{calc} = 3.504$ Å; $c_{calc}/a_{calc} = 1.142$, with the experimental data [23], $a = 3.085$ Å; $c = 3.523$ Å; $c/a = 1.142$ (the deviations are 0.52% and 0.53%, respectively).

Changes in chemical bonding upon incorporation of a dopant atom into a Mg-site was studied in terms of charge-density distributions. In order to characterize variations of the partial charges at the magnesium position upon substitution and to assign a specific meaning of ionic charges in the analysis, values of the Bader effective charges [35] have been evaluated. Their calculations were carried out by using software [36], which utilizes a grid-based Bader analysis algorithm [37]. The contribution of local many-body polarization effects was analyzed in terms of the Born effective charges, values of which have been obtained by using the special extended method adopted at VASP.

3. Results

In tables 2 to 5, we present the main results which characterize the influence of the Zn, Cu and Zr substitutional impurities on displacements of the boron atoms, the electronic charge redistribution around a cation, and the local properties of chemical bonding in MgB_2. These results and several consequences of magnesium replacement are discussed below. The main conclusions are summarized at the end of the paper.

3.1. Characterization of local distortions

We pay attention to the data of table 2 as they reveal certain trends. First, no significant changes are seen – local lattice distortions, and the induced changes in transverse ionic strengths caused by cationic substitution appear to be notably small. Particularly, this observation relates to cases with Cu and Zn. This implies that the relevant bond lengths are preserved, and the boron layer remains planar. Further, it is also seen from table 2 that longitudinal (in-plane) stresses are more strongly affected by the impurities, though the induced changes remain relatively small.

The overall comparison of the data of table 1 with the simulation results of table 2 reveals a certain correlation between the variation in the magnitude of the T_c suppression rate ($\Delta T_c/\Delta x$) and the doping induced changes in the boron sublattice. This can be emphasized by observing the following difference: While in the majority of the doped solutions, the presence of several percents of divalent impurity metal atoms provides

Table 2. Calculated lattice distortions and changes of interatomic forces in the boron layer caused by substitutional impurities in the magnesium diboride[a].

Host/Imp. cation	B out (Å)	B in (Å)	force components along c-axis (eV/Å)	in a-b plane (eV/Å)
Mg	0	0	0	0
Zn	+0.0045	−0.0054	+0.020	−0.089
Cu	−0.0002	−0.0128	−0.014	−0.234
Zr	−0.0063	+0.0159	−0.013	+0.260

[a]Denoted: 'B out/B in' – boron out-of/in-plane displacement as shown in figure 1; the minus sign indicates inward directions.

already a considerable suppression of T_c, there are substitutions such as Zn, Cu, or even tetravalent Zr low concentrations of which slightly influence both the superconducting order and the specific positions of the boron atoms. The reason for this discrepancy seems to be related primarily to the strong 2D B-B linkage dominating in the boron layer [38] which, as we have shown above, tends to keep the existing structural stability upon a change in the host cation. Considering Mg as a reference cation, another interesting result is that one may say according to [3, 39] that the incorporation of just Zn, Cu or Zr into the Mg-site has little effect on actual interband pairing channels. Correspondingly, in these cases, the protection function of the covalent boron linkage cannot be markedly influenced (at low doping levels) what may provide a much weaker dependence of the superconducting temperature T_c on impurity content.

3.2. Characterization of dopant local bonding

In order to get further insight into why the substitutional Zn, Cu and Zr cause only minor changes in a planar geometry of the covalent boron layer, we undertook an investigation of how local properties of chemical bonding are affected by the overall electronic structure and elemental characteristics of each of the considered impurity ions. For characterization of impurity-induced changes in chemical bonding via the differences of the electron states between the host and foreign cations, we performed an extensive comparative analysis of the relevant charge partitioning schemes. Figure 2 shows charge density maps calculated for MgB_2 and all three doped cases; the maps are projected onto the (100) plane and contain the central Mg or M = Zn, Cu, Zr cations, and surrounding B atoms. Figure 3 is instructive in another way: for each cation considered, it shows the line charge density distributions along the Mg-B and M-B directions, respectively. Computed values of the Bader effective charges (Q_B) presented in table 3 reflect the topology features of the underlying electron-density distribution emerging as a direct consequence of the relevant arrangements. Comparison of figures 2, 3 and the data of table 3 for the reference case of the Mg(II) ion reproduces the

Table 3. Some charge characteristics related to the host cation and its substituents in the magnesium diboride. The Pauling electronegativities are taken from [40]. The quantities $Q_B(M)$ denote Bader effective charges calculated from electronic densities (in units of $|e|$).

	Mg	Zn	Cu	Zr
Electronegativity difference values with respect to boron	0.73	0.39	0.14	0.71
$Q_B(M)$	+2.0	+0.69	+0.42	+2.68[a]

[a]A comparison shows that this value appears to be equal to that of +2.67 obtained from the self-consistent LAPW calculations for the bulk zirconium diboride ZrB_2 [41].

well-established result [2, 23, 42, 43, 44, 45] that Mg is an ionically-bonded cation (with an admix of some weak covalency) in a stable divalent state.

Analysis of cases where Zn or Cu substitutes for Mg revealed three significant differences. First, as depicted in table 3, the Bader effective charges are quite different from the formal chemical charge +2. Two other differences are very clearly delineated on figures 2 and 3; common to both ions they are: a depletion of the electron charge along the metal-boron bonding direction, and a large degree of electron charge accumulation of fairly good spherical form around the nuclei. Correspondingly, the physical picture of the outer electronic structure of Zn and Cu incorporated into magnesium diboride can be drawn as follows: (i) the 3d states appear to be completely filled (what provides increased electron density at the substituent, causes the observed spherical charge distribution around it, and induces the smaller effective charge transfer, in comparison with magnesium), (ii) zinc and copper cations acquire fractional quantities of the 4s electron populations, about 1.31e and 0.58e, respectively, (iii) the partially filled 4s states constitute the resulting outermost orbitals, and (iv) the d-electron covalency effects are extremely low because the filled 3d levels of the substituent are shielded by its 4s states. Remarkably, smallness of the effective charges relative to the nominal chemical valence +2 is an indication of the fact that the substitutional cations have retracted the certain amount of the delocalized electrons that participate in metallic bonds. The reason why just the electrons shared by the boron atoms are excepted is that the significant changes in an equilibrium planar geometry of the covalent boron layer are absent. Furthermore, of note is another observation from table 3 that the local loss of charge exchange activity is directly connected with the drop in the electronegativity difference with respect to boron in the series of elements Mg, Zn, Cu.

It may be concluded thus that both substitutions give rise to a negative tendency which manifests itself (i) in increasing the electron density around outer orbitals of the Zn or Cu cations, and (ii) in decreasing the positive charge at the cation center up to the values of $Q_B(Zn) = +0.69$ and $Q_B(Cu) = +0.42$, respectively. This leads to partial neutralization of the overall charge on the substituents, makes the initial charge transfer channels much weaker and therefore causes the significant reduction of

the polar contribution into the cationic nature of the substitutional ion. As a result, the initial, predominantly ionic character of the local environment is degraded. The variances of the Bader effective charges from the nominal +2 may therefore be regarded as a degree of Zn or Cu "underbonding" that should have a certain effect on physical properties of MgB_2 doped by these elements. For example, since the interband channel is unaltered (because of minor changes in a planar geometry of the covalent boron layer), the experimentally observed smallness of suppression of the superconducting temperature is perfectly understandable via influence of the above-mentioned retraction of "previously expelled electrons" on the density of electronic states at the Fermi level. This result correlates well with the conclusion made in [46] for a series of Al-Li codoped MgB_2 systems that the superconductivity is much more affected by the relevant lattice distortion induced by impurity ion substitution than by the band filling.

The trend towards electron density accumulation and a weakening of charge transfer channels breaks down for the case of the substitutional Zr in the structure of MgB_2. Although Zr possesses almost the same electronegativity difference as Mg , the calculated value of the Bader effective charge, $Q_B(Zr) = +2.68$, is considerably different from the formal valence 4+. From chemical point of view, this implies that the zirconium cation in the MgB_2 lattice tends towards a lower oxidation state‡. In contrast to zinc and copper ions, Zr attempts to expand definite amounts of charge density from itself toward an interstitial area. Analysis of figures 2 and 3 strongly suggests the moderate enhancement of the positive charge on the cation which takes place due to delocalization of its 4d electrons caused by partial donation of 0.68 additional electrons. Such a delivery of a partial charge (along the metal–non-metal charge-transfer configuration) is well correlated with a chemical readiness of the zirconium cation to give up the valence 4d electrons in order to move back to the predominant oxidation state of 4+ and to activate the covalent bonding with neighboring atoms. Consequently, as compared with the parent compound MgB_2, an ionization increase $Mg^{2+} \rightarrow Zr^{2.68+}$ on a substitutional cation site and the presence of appreciable covalency in the same region may give rise to a tendency towards dielectrization of the system. This observation is confirmed by first-principles studies of the bulk compound ZrB_2 [45, 48, 49], which show the presence the strong hybridization between the Zr 4d and the B 2p states as well as drastic fall of the density of electronic states at the Fermi level.

Thus, we can conclude that electronic charge distribution at the Mg position in the bulk magnesium diboride is very sensitive to the cation replacement. Firstly, the substitution for an impurity ion of the same nominal charge +2 leads to a substantial charge redistribution around the cation. Secondly, the change in the chemical bonding character depends on the type of metal ion and its electronegativity versus boron, so that among substitutional ions considered two different trends can be distinguished. All this underlines in the light of the bonding situation that ion substitution not only always affects the existing chemical bonds but also that the resulting charge rearrangement is

‡ This point suggests the presence of some mechanism of valence reduction upon substitution, as can be compared with $4d^2$ configurations of low-valent Zr(II) in complex sheet and cluster structures [47].

exhibited quite differently for the cations considered in the present work. Moreover, in the context of superconductivity, these features can seriously limit the targeting efficiency of a number of potential substituents or even make them unfavorable towards the enhancement of superconducting properties.

3.3. Pressure effects

To complete the results obtained for impurity-induced changes in the cation charge states, it should be interesting to study how these changes proceed under pressure. For this purpose, the Zr- and Zn-doped case were considered. We employed the same set of calculations as used throughout this work and fully relaxed a doped system. The resulting pictures of the charge density maps are shown in figure 4. The comparison of the charge distributions with those shown in figure 2 reveals no significant changes between them. The most remarkable difference is a slight increase of the Bader effective charge of the Zr cation – from +2.68 at zero pressure to +2.84 under pressure of 16.5 GPa (what evidently indicates the above-mentioned oxidation tendency to the tetravalent state). This implies that the charge state of Zr remains relatively stable with compression until at least 16.5 GPa.

The Zn substitutional cation also demonstrates the similar tendency to maintain its charge state under pressure. For example, the calculated change in the Bader effective charge under compression of 14.7 GPa, $\Delta Q_B(Zn) = +0.04$, shows that due to contraction of the filled 3d levels, valence electrons do not favor extra oxidation. As a result, the overall charge configuration of Zn in magnesium diboride is essentially unaffected by pressure.

3.4. The Born effective charges

Another possible microscopic reason of lattice distortions stems from the fact well-known in the theory of local phase transitions that distortion of local geometry around an impurity may be caused by sufficient strength of the purely dynamical part of the charge transfer (e.g., [50, 51]). Generally speaking, significance of dynamical charge transfer processes generated by vibronic mixing of the proper electronic states is one of most important characteristic features of polar crystals [52, 53, 54, 55]. On the atomic level, this feature is associated with many-body polarization effects that contribute to ionic dipole polarization, and it reflects a mixed ionic(polar)-covalent character of the relevant chemical bonds [55]. Since the latter can be interpreted in terms of the Born dynamic effective charges with respect to some reference (nominal) ionic value (e.g., [56, 55]), the calculations of the principal values of the Born dynamic effective charge tensor Z^* can be employed as a test of how electronic effects of the many-body nature translate the polar contribution into ionic chemical bonding. It is also of note that although the idea of calculation of the Born dynamic effective charges for a conducting material may seem senseless at first glance, it can be, due to logic behind the ionic bonds and charge

Table 4. Principal values of the Born effective charge of Mg(II) in magnesium diboride (in units of $|e|$). The diagonal form with $Z^*_{xx}(Mg) = Z^*_{yy}(Mg)$ reflects hexagonal symmetry of the tensor $Z^*(Mg)$. The quantity $\bar{Z}^*(Mg)$ represents the average over crystal axes: $\bar{Z}^*(Mg) = (1/3)(Z^*_{xx}(Mg) + Z^*_{yy}(Mg) + Z^*_{zz}(Mg))$.

$Z^*_{xx}(Mg)$	$Z^*_{yy}(Mg)$	$Z^*_{zz}(Mg)$	$\bar{Z}^*(Mg)$
+1.87	+1.87	+2.31	+2.02

transfer, reasonably useful for a mixed bonded solid, indicating how specific pieces of a composite picture of chemical bonding may be distinguished.

In table 4, we have presented the converged values of the Born effective charge for the magnesium cation in MgB_2 (due to metallic properties of MgB_2, we focused on dynamic charges only for cations and not for boron atoms). It may be assumed that the numerical convergence to stable values of table 4 is guaranteed by the nearly ionic character of the Mg sublattice which, in the spirit of layered superconductivity approach [57, 58], can be figuratively imagined as a stack of the intrinsic insulating layers. Calculations have also predicted principal values of the electronic dielectric constant for the bulk magnesium diboride: $\epsilon^{xx}_{\infty} = \epsilon^{yy}_{\infty} = 22.45$, $\epsilon^{zz}_{\infty} = 5.77$. The theoretical value $\epsilon_{\infty} = 16.9$, evaluated as an average $\epsilon_{\infty} = (1/3)\Sigma_i \epsilon^{ii}_{\infty}$, is quite comparable with the experimental estimate of 11.9 [8] thus proving the consistency of the present analysis.

The tensorial nature of the Born effective charge provides subtle information concerning differences in directions and strengths of dynamical processes related to the ionic sites and caused by the polarization effects. As seen by comparing the values of table 4, there exists a certain anisotropy, as is indicated by the observation that in the directions perpendicular (the *ab*-plane) and parallel to the *c*-axis the components of the dynamic charge differ markedly from the formal value of 2+. This suggests that, although on the average Mg remains quite well ionized in the full N-particle ensemble ($\bar{Z}^*(Mg) = +2.02$), (i) the attached effective potential, which gives rise to polarization force fields acting in a local environment around magnesium, appears non-spherical, and (ii) due to deviation from the nominal ionic charge some contribution of the pure dynamic covalent nature in the magnesium–boron bonding should be assumed. The latter is entirely consistent with previous studies of dynamical covalency effects in MgB_2 [59].

In order to analyze how the change in the host cation influences the attached effective potential, we carried out the relevant calculations of the Born effective charges for the substitutional impurities we are considering here. In contrast to the previous case of magnesium, the computational method failed to give uniform results consistent with hexagonal symmetry. In the physical sense, the lack of numerical consistency is not discouraging, and should be considered as an additional confirmation of the drastic changes of a charge state which arise around the host cation position due to its replacement. In other words, impact of the substitutions with such unavoidable outcomes as falling of ionic character of chemical bonding, and the expansion of a

Table 5. The averaged principal values of the Born effective charge tensor for the foreign cation M = Zn,Cu,Zr in magnesium diboride (in units of $|e|$). $\bar{Z}^{*(avg)}(M) = (1/3)(Z_{xx}^{*(avg)}(M) + Z_{yy}^{*(avg)}(M) + Z_{zz}^{*(avg)}(M))$.

	$Z_{xx}^{*(avg)}(M)$	$Z_{yy}^{*(avg)}(M)$	$Z_{zz}^{*(avg)}(M)$	$\bar{Z}^{*(avg)}(M)$
Zn	+1.6617	+1.6617	+2.25	+1.86
Cu	+1.1378	+1.1345	+1.85	+1.38
Zr	+1.4018	+1.4630	+2.26	+1.71

metallic environment beyond the range of the boron layers [45, 48] make it impossible to get from the method of calculations the target values of dynamic charges for the foreign cations. To obtain some approximate estimates of the Born effective charges, we have constructed a smooth procedure based on averaging the obtained results over the supercell, so that all the cations employed in the calculations are taken into account. This can be done since overall charge balance is maintained. Due to electroneutrality of the simulation supercell, one can then expect that summation eliminates off-diagonal contributions, suppresses discontinuities, random perturbations and other artificial symmetry effects and thus will return the weighted-average components of the Born effective charge tensor in the original diagonal form.

In table 5, we have presented the numerical values of the dynamic charges for Zn, Cu and Zr substitutional cations as averages over the supercell. It is seen that the remaining uncertainties on the averaged values of charges are really negligible, so that this type of approximation is quite reasonable. Nevertheless, one additional aspect which should be discussed here is the sensitivity of the retrieval accuracy within such a calculation procedure. First of all, we note that all off-diagonal contributions are exactly eliminated. On the other hand, the required identity of the diagonal terms ($Z_{xx}^{*(avg)} = Z_{yy}^{*(avg)}$) is restored at different accuracy levels: for zinc and copper, we get a more accurate retrieval than for zirconium. We believe that this result is not surprising because some discrepancy in the case of zirconium suggests that due to the expansion of metallic bonds into the cationic environment, the effect of charge fluctuations is not completely eliminated after summation over the supercell.

The results listed in table 5 allow us to characterize the specific features of chemical bonds in terms of the Born effective charges as follows. (i) A dynamic component in resulting chemical bonding becomes smaller upon cation substitution (as compared with that of Mg), and (ii) this partial loss in initial dynamic covalency is caused by the relevant charge redistribution around the cation position. At the same time, as seen from table 5, a rate of an anisotropy in the dynamics of valence charge distribution remains relatively unchanged in the cases of zinc and zirconium. Moreover, of all three components just the z component of the Born effective charge, which is particularly interesting for dynamical covalency effects in magnesium diboride, tends to be close to the c-axis value of the Mg cation and therefore appears, in comparison with in-plane

x, y components, to be more robust to alteration of charge densities. Following the same consideration as in [60], this leads us to an understanding regarding why lattice distortions induced by Zn, Cu or Zr ions are so small: the explanation is that the ionic strength changes induced by variations of dynamical charge transfer along the c-axis are not large enough to drive the relative boron displacements.

4. Conclusions

In order to understand the leading factors that govern adjustments of the lattice positions during accommodating the foreign cation in MgB_2, we investigated the induced deformations (lattice distortions) in the local geometry of the boron sites. The first-principles calculations were performed for three different substitutional cations such as divalent Zn(II) and Cu(II), and tetravalent Zr(IV). These species are of particular interest because they demonstrate the lowest-observed-droop of the superconducting temperature among most of the impurities of the same formal valences. Inspection of the relaxed lattice structures together with the results of the performed calculations allowed the following conclusions to be drawn: (i) At a low doping level, the Zn, Cu and Zr substitutions cause only negligible changes in the structural arrangement of the neighboring boron atoms. (ii) Such an insignificant impact on the local geometry of the boron layer is mostly attributed to two aspects. The first is the observation that the existing in-plane B-B covalent bonding is strong enough to keep effectively the boron atoms non-shifted under substitution of magnesium with Zn, Cu or Zr. The second is that dynamical covalency processes along the cation-boron bonding tend to be tolerant of changes in the host cation and, consequently, cannot create a channel of instability in the boron layer. Both aspects are important in view of the fact that the structural balance between local geometry and chemical bonding are related to the electron structure of the impurity and to the bonding connections carried out by the impurity. (iii) A role of small deformations of the local geometry of the boron layer induced by the impurity ions may be insufficient to influence alone on superconductivity of the host system. (iv) Generally, our results emphasize that MgB_2 is the perfect material having a unique combination of an ideal planar layer structure, the predominantly ionic character of the cationic sublattice, and the high degree of chemical bonding stability.

In order to investigate the characteristic measures of impurity activity, such as charge states and the impurity-induced changes in the chemical bonding, we performed the comparison analysis of the underlying charge-transfer processes. It has been discovered that the replacement of Mg(II) by divalent Zn(II), Cu(II) or tetravalent Zr(IV) influences substantially the character of the charge transfer, so that the distributions of the charge around the impurities and degree of ionicity differ drastically both from that around the host cation and also from each other. It has been shown that the different cationic nature of the substituents dictates two entirely opposite directions along which the induced changes in the local structure take place. First, the change in the host cation leads to density contraction – the substitutional Zn or Cu demonstrate

the considerable increase of the overall charge density due to retaining its valence electrons and the small amount of charge transfer to the boron layers. Particularly, a larger accumulation of a charge and the least charge transfer are observed for the copper ion. It was argued that this process retracts the certain amount of the delocalized electrons from metallic bonds what causes the observed decrease in the superconducting temperature values as the substitution level grows. Second, the change in the host cation leads to charge delocalization – no charge accumulation is observed for Zr. The Zr incorporation into the Mg site of MgB_2 tends (a) to preserve the initial charge transfer channels, and (b) by partial donation of 4d electrons to add some amounts of ionicity and covalency into the local cation-anion coupling. It was suggested that such increasing of covalency character does not favor superconducting properties of the host material. The stability of charge states related to the impurity cations was tested against pressure: the pressure dependence of the charge transfer degree was found to be very weak. The theoretically observed effective charges indicate that the substitutional ions do not possess their formal valence (oxidation state), and are characterized by different levels of electron delocalization; zirconium as an electron donor is indeed stronger than magnesium. As a consequence, by comparison with less positively charged zinc and copper, the behavior of zirconium remains much more tolerant (affine) to the usual ionic distribution associated with the host magnesium cation.

Summing up, one can say that the induced local lattice distortions and changes of the charge transfer degree may serve as structurally sensitive prognostic parameters for signaling how the superconductivity in MgB_2-solid solutions is affected by impurities, for clarifying the functional roles and efficiency of such various factors as a geometry of the boron layer, the electronegativity difference, ionic character of the local environment, relative affinities toward magnesium and boron, etc., and on this basis for facilitating more precise theoretical predictions in synthesis and characterization.

Acknowledgments

The authors are grateful to Professor N. Kristoffel for suggesting the subject of this paper and for numerous helpful discussions and constructive comments.

This work was supported by the European Union through the European Regional Development Fund (Centre of Excellence "Mesosystems: Theory and Applications", TK114). It was also supported by the Estonian Science Foundation grant No 7296.

References

[1] Buzea C and Yamashita T 2001 *Supercond. Sci. Technol.* **14** R115
[2] Ravindran P, Vajeeston P, Vidya R, Kjekshus A and Fjellvåg H 2001 *Phys. Rev.* B **64** 224509
[3] Erwin S C and Mazin I I 2003 *Phys. Rev.* B **68** 132505
[4] Ivanovskii A L 2003 *Fiz. Tverdogo Tela* **45** 1742 Engl. Trans.: 2003 *Phys. Solid State* **45** 1829
[5] Cava R J, Zandbergen H W and Inumaru K 2003 *Physica* C **385** 8
[6] Singh P P 2003 *Bull. Mater. Sci.* **26** 131

[7] Bernardini F and Massidda S 2006 *Europhys. Lett.* **76** 491
[8] Di Castro D, Ortolani M, Cappelluti E, Schade U, Zhigadlo N D and Karpinski J 2006 *Phys. Rev.* B **73**, 174509
[9] Kortus J 2007 *Physica* C **456** 54
[10] Kuzmenko A B 2007 *Physica* C **456** 63
[11] Li W X, Zeng R, Poh C K, Li Y and Dou S X 2010 *J. Phys.: Condens. Matter* **22** 135701
[12] Ojha N, Malik V K, Singla Rashmi, Bernhard C and Varma G D 2010 *Supercond. Sci. Technol.* **23** 045005
[13] Singh P P 2002 *Physica* C **382** 381
[14] Moritomo Y and Xu Sh 2001 ArXive: cond-mat/0104568v1
[15] Kazakov S M, Angst M, Karpinski J, Fita I M and Puzniak R 2001 *Solid State Commun.* **119** 1
[16] Tampieri A, Celotti G., Sprio S, Rinaldi D, Barucca G and Caciuffo R 2002 *Solid State Commun.* **121** 497
[17] Singh K, Mohan R, Shelke V, Gaur N K and Singh R K 2008 *Indian J. Pure & Appl. Phys.* **46** 420
[18] Kalavathi S and Divakar C 2005 *Bull. Mater. Sci.* **28** 249
[19] Feng Y, Zhao Y, Yan G, Pradhan A K, Zhou L, Koshizuka N and Murakami M 2004 Critical Current Density, Flux Pinning and Microstructure in MgB_2 Superconductors *High Temperature Superconductivity 1 Materials* ed A V Narlikar (Berlin, Heidelberg: Springer-Verlag) pp. 401-430
[20] Sun Y, Yu D, Liu Z, He J, Zhang X, Tian Y, Xiang J and Zheng D 2007 Appl. Phys. Lett. **90** 052507
[21] Shi L, Zhang S and Zhang H 2008 *Solid State Commun.* **147** 27
[22] M'chirgui A, Ben Azzouz F, Annabi M, Zouaoui M and Ben Salem M 2005 *Solid State Commun.* **133** 321
[23] Mazin I I and Antropov V P 2003 *Physica* C **385** 49
[24] Kristoffel N, Örd T and Rägo K 2003 *Europhys. Lett.* **61** 109
[25] Kristoffel N, Örd T and Rägo K 2003 *J. Supercond.* **16** 517
[26] Bussmann-Holder A and Bianconi A 2003 *Phys. Rev.* B **67** 132509
[27] Kresse G and Hafner J 1993 *Phys. Rev.* B **47** 558
[28] Kresse G and Hafner J 1994 *Phys. Rev.* B **49** 14251
[29] Kresse G and Furthmüller J 1996 *Comput. Mater. Sci.* 6 , 15
[30] Kresse G and Furthmüller J 1996 *Phys. Rev.* B **54** 11169
[31] Blöchl P E 1994 *Phys. Rev.* B **50** 17953
[32] Kresse G and Joubert D 1999 *Phys. Rev.* B **59** 1758
[33] Perdew J P, Burke K and Ernzerhof M 1996 *Phys. Rev. Lett.* **77** 3865; 1997 *Phys. Rev. Lett.* **78** 1396
[34] Monkhorst H J and Pack J D 1976 *Phys. Rev.* B **13** 5188
[35] Bader R F W 1990 Atoms in Molecules: A Quantum Theory (Oxford: Oxford University Press)
[36] http://theory.cm.utexas.edu/vtsttools/bader
[37] W. Tang, E. Sanville, G. Henkelman 2009 *J. Phys.: Condens. Matter* **21** 084204
[38] Choi H J, Roundy D, Sun H, Cohen M L and Louie S G 2002 *Nature* **418** 758
[39] Mitrovič B 2004 *J. Phys.: Condens. Matter* **16** 9013
[40] Barbalace K 1995-2011 *Periodic Table of Elements* (EnvironmentalChemistry.com)
[41] Switendick A C 1990 Electronic structure and charge density of zirconium diboride *Technical Report* SAND–90-1474C; CONF-900870–7
[42] An J M and Pickett W E 2001 *Phys. Rev. Lett.* **86** 4366
[43] Kortus J, Mazin I I, Belashchenko K D, Antropov V P and Boyer L L 2001 *Phys. Rev. Lett.* **86** 4656
[44] Belashchenko K D, van Schilfgaarde M and Antropov V P 2001 *Phys. Rev.* B **64** 092503
[45] De La Mora P, Castro M and Tavizón G 2002 *J. Sol. Stat. Chem.* **169** 168
[46] Monni M, Ferdeghini C, Putti M, Manfrinetti P, Palenzona A, Affronte M, Postorino P,

Lavagnini M, Sacchetti A, Di Castro D, Sacchetti F, Petrillo C and Orecchini A 2006 *Phys. Rev.* B **73** 214508

[47] Kalvins A K 1985 A review of the inorganic and organometallic chemistry of zirconium *Report No 85-124-K*

[48] Shein I R and Ivanovskii A L 2002 *Fiz. Tverdogo Tela* **44** 1752 Engl. Trans.: 2002 *Phys. Solid State* **44** 1833

[49] Rosner H, An J M, Pickett W E and Drechsler S-L 2002 *Phys. Rev.* B **66** 024521

[50] Kristoffel N 2000 Structural distortions and oxygen local dynamic instabilities in superconducting perovskites *Defects and Surface-Induced Effects in Advanced Perovskites* (*NATO Science Series 3. High Technology*) ed G Borstel, A Krumins and D Millers (Dordrecht: Kluwer Scientific Publishers) pp. 113-124

[51] Kristoffel N and Klopov M 1996 *Phys. Rev.* B **54** 9074

[52] Kristoffel N N 1984 *Czech. J. Phys.* B **34** 1253

[53] Kristoffel N and Konsin P 1988 *Phys. Status Solidi* (b) **149** 11

[54] Bussmann-Holder A, Bilz H and Benedek G 1989 *Phys. Rev.* B **39** 9214

[55] Pishtshev A 2011 *Physica* B **406** 1586

[56] Lee K W and Pickett W E 2003 *Phys. Rev.* B **68** 085308

[57] Bill A, Morawitz H and Kresin V Z 2003 *Phys. Rev.* B **68** 144519

[58] Varshney D, Azad M S and Singh R K 2004 *Supercond. Sci. Technol.* **17** 1446
Varshney D, Nagar M, Bhatnagar S and Varshney M 2010 *Supercond. Sci. Technol.* **23** 075016

[59] Deng S, Simon A and Köhler J 2005 Pairing Mechanisms Viewed from Physics and Chemistry *Superconductivity in Complex Systems* (*Structure and Bonding vol 114*) ed K A Müller and A Bussmann-Holder (Berlin, Heidelberg: Springer-Verlag) pp. 103-141

[60] Ghosez Ph and Veithen M 2007 *J. Phys.: Condens. Matter* **19** 096002

Figure Captions:

Figure 1: A bulk 81-atoms supercell modeling the $M_xMg_{1-x}B_2$ composition for $x = 0.037$. The MgB_2 cell containing the impurity cation is sketched. In-plane and out-of-plane boron displacements are indicated by arrows.

Figure 2: Charge density maps of (a) MgB_2, (b) $Zn_{0.037}Mg_{0.963}B_2$, (c) $Cu_{0.037}Mg_{0.963}B_2$ and (d) $Zr_{0.037}Mg_{0.963}B_2$ projected onto the (100) plane.

Figure 3: Comparison of the line charge density distributions calculated along the cation-anion direction. The dashed, dot-and-dash and solid curves represent Zr-substituted, Cu-substituted and Zn-substituted MgB_2, respectively. The inset shows the corresponding profile for the non-substituted MgB_2.

Figure 4: Charge density maps of (a) Zr-substituted and (b) Zn-substituted MgB_2 projected onto the (100) plane. Calculations were made for a pressure of 16.5 GPa and 14.7 GPa, respectively.

Figures

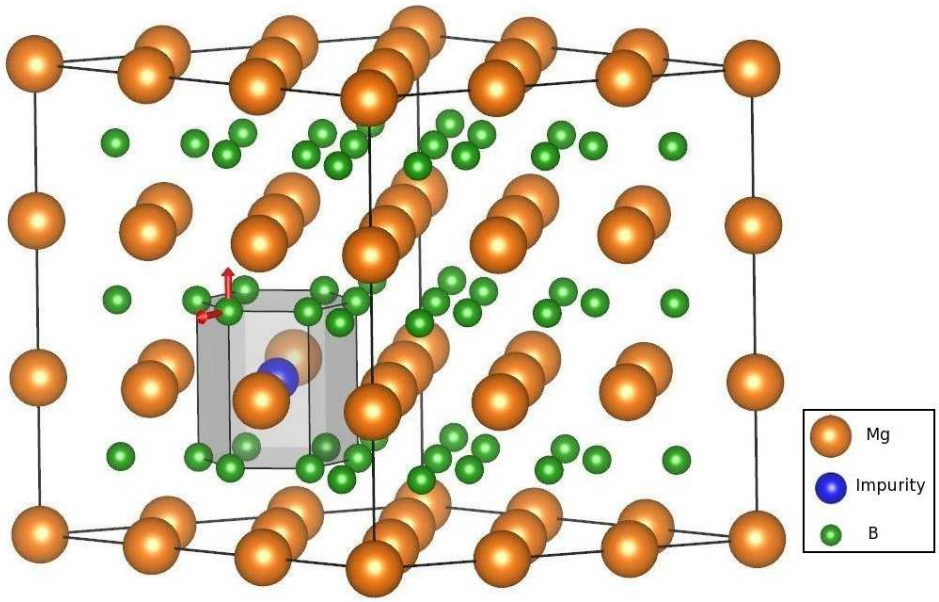

Figure 1. A bulk 81-atoms supercell modeling the $M_xMg_{1-x}B_2$ composition for $x = 0.037$. The MgB_2 cell containing the impurity cation is sketched. In-plane and out-of-plane boron displacements are indicated by arrows.

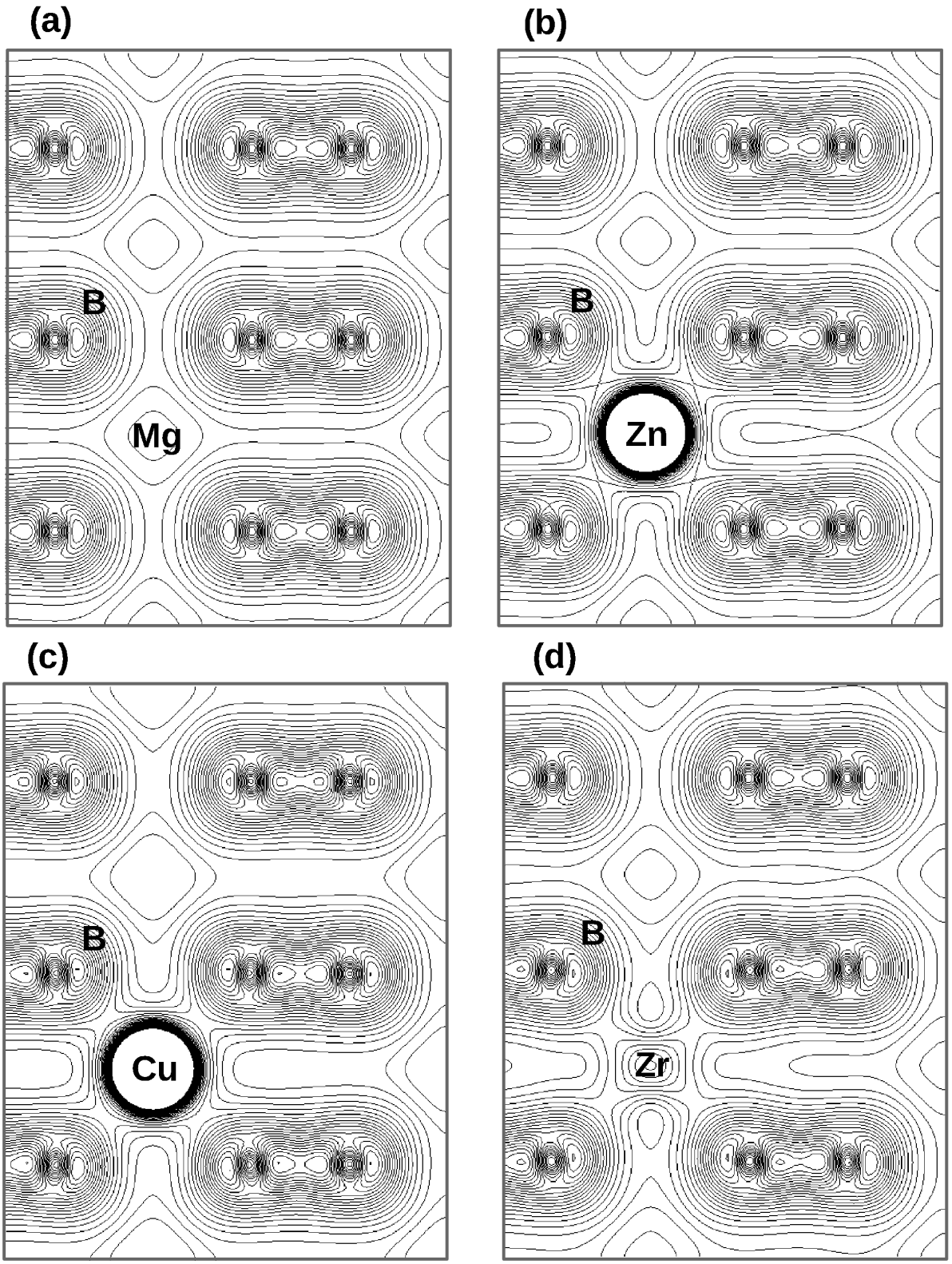

Figure 2. Charge density maps of (a) MgB_2, (b) $Zn_{0.037}Mg_{0.963}B_2$, (c) $Cu_{0.037}Mg_{0.963}B_2$ and (d) $Zr_{0.037}Mg_{0.963}B_2$ projected onto the (100) plane.

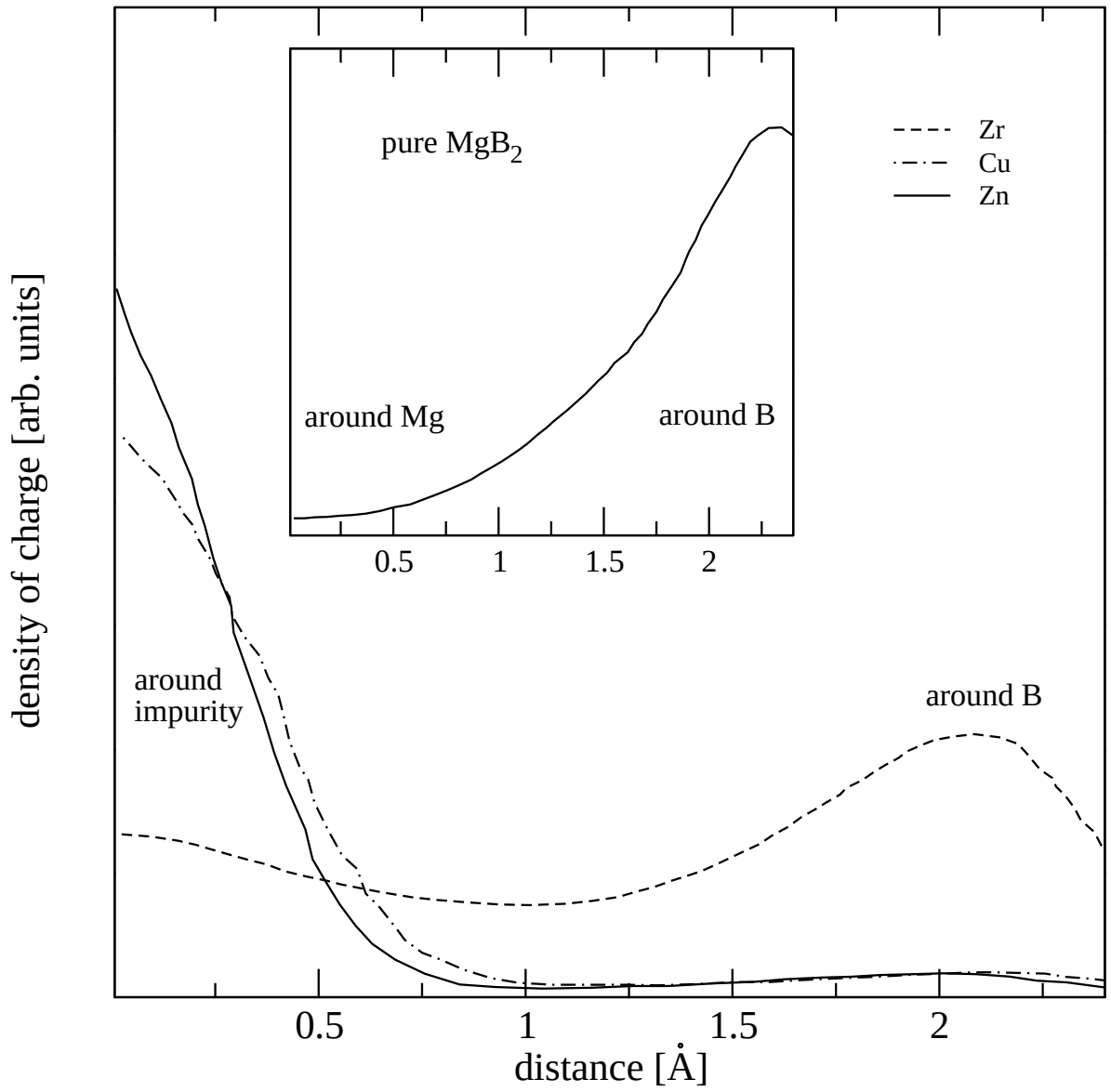

Figure 3. Comparison of the line charge density distributions calculated along the cation-anion direction. The dashed, dot-and-dash and solid curves represent Zr-substituted, Cu-substituted and Zn-substituted MgB_2, respectively. The inset shows the corresponding profile for the non-substituted MgB_2.

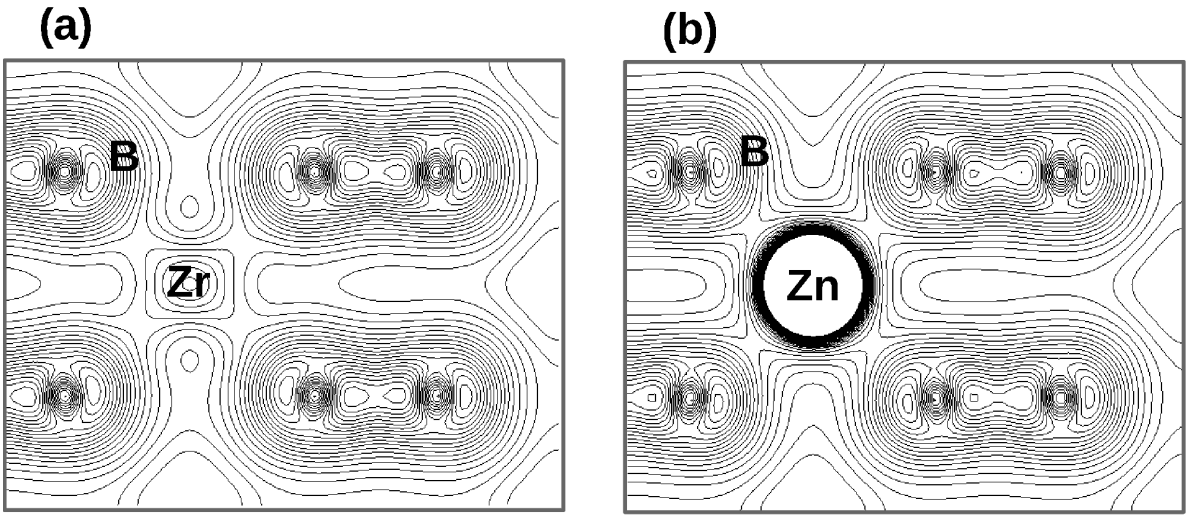

Figure 4. Charge density maps of (a) Zr-substituted and (b) Zn-substituted MgB_2 projected onto the (100) plane. Calculations were made for a pressure of 16.5 GPa and 14.7 GPa, respectively.